IEEE Photonics Journal
An IEEE Photonics Society Publication

Open Access

Emulation of Spiking Response and Spiking Frequency Property in VCSEL-Based Photonic Neuron

Volume 8, Number 5, October 2016

Shuiying Xiang
Aijun Wen
Wei Pan

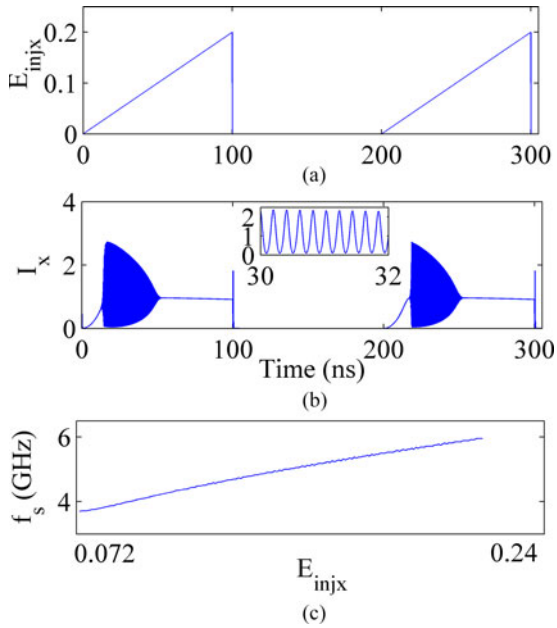

DOI: 10.1109/JPHOT.2016.2614104
1943-0655 © 2016 IEEE

Emulation of Spiking Response and Spiking Frequency Property in VCSEL-Based Photonic Neuron

Shuiying Xiang,[1,2] **Aijun Wen,**[1] **and Wei Pan**[3]

[1]State Key Laboratory of Integrated Services Networks, Xidian University, Xi'an 710071, China
[2]State Key Discipline Laboratory of Wide Bandgap Semiconductor Technology, School of Microelectronics N, Xidian University, Xi'an 710071, China
[3]School of Information Science and Technology, Southwest Jiaotong University, Chengdu 610031, China

DOI:10.1109/JPHOT.2016.2614104

Manuscript received June 29, 2016; revised September 6, 2016; accepted September 23, 2016. Date of publication September 27, 2016; date of current version October 13, 2016. This work was supported in part by the National Natural Science Foundation of China under Grant 61674119, Grant 6130606, and Grant 61274042; in part by the Postdoctoral Innovation Talent Program in China under Grant BX201600118; in part by the Young Talent fund of University Association for Science and Technology in Shaanxi, China, under Grant 20160109; in part by the China 111 Project under Grant B08038; and in part by the Specialized Research Fund for the Doctoral Program of Higher Education of China under Grant 20130203120001. Corresponding author: S. Xiang (e-mail: jxxsy@126.com).

Abstract: The dynamical response properties of photonic neuron based on vertical-cavity surface emitting lasers (VCSELs) subject to orthogonal polarized optical pulse injection stimuli have been numerically investigated. Based on the well-known spin flip model, we first reproduce some experimental findings of neuron-like dynamics in VCSELs, such as phasic spiking with a single abrupt pulse, and tonic spiking with multiple periodic pulses. Besides, we further go beyond in three directions and obtain several novel results. The operating parameter ranges corresponding to different neuron-like dynamics are identified by extensive bifurcation analysis. In addition, the effect of the time-varying pump current on the neuron-like dynamics for VCSELs under given optical injecting pulse strength is also discussed. For a given pump current, the spiking frequency dependence on the stimuli strength is further revealed in VCSELs with time-varying optical pulse injection. Such controllable neuron-like response dynamics and spiking frequency dependence in VCSELs are interesting and valuable for ultrafast photonic neuromorphic systems and neuron-inspired photonic information processing.

Index Terms: Vertical-cavity surface-emitting lasers (VCSELs), polarization, photonic neuron, spiking frequency dependence.

1. Introduction

Photonics technology has attracted growing interest in brain-inspired neuromorphic computing systems in recent years, due to the inherit advantages of high speed, wide bandwidth, and low electromagnetic interference [1]–[5]. Many types of lasers and configurations, such as semiconductor lasers with optical injection/feedback [6]–[8] or with saturable absorber [9], semiconductor ring lasers [10], semiconductor micro-disk lasers [11], and optoelectronic oscillators [12], have been adopted to mimic successfully the dynamic response of biological neuron but at a much faster time scale.

Compared to conventional semiconductor lasers, vertical-cavity surface emitting lasers (VCSELs) are promising candidates for many potential applications as they exhibit many profound advantages such as, low cost, ease to integrate in 2-D array, and high coupling efficiency to optical fiber. In particular, two orthogonal polarizations, denoted as X-polarization (XP) and Y-polarization (YP) modes may be coexisted, and the polarization-related properties of VCSELs subject to parallel or orthogonal polarized injection have attracted much attention [13]–[22].

Recently, Hurtado *et al.* have experimentally reported emulation of neuronal responses based on the polarization dynamics and nonlinear dynamics induced in VCSELs under polarized optical injection [23]–[25]. Furthermore, controllable and reproducible spiking patterns, including single and multiple pulses responses, have been experimentally obtained in VCSELs under different cases of polarized injection (parallel and orthogonal) of modulated temporal signals [24]–[25]. While a detailed numerical bifurcation analysis of neuron-like dynamics in VCSELs is still an interesting topic that remains largely unexplored. Besides, in some spiking laser systems, it has been shown experimentally and theoretically that the spiking frequency was increased with the stimuli strength [26]–[27], which is similar to a well-know property in neural system [28]. However, such spiking frequency dependence has yet to be reported in a photonic neuron based on VCSELs with orthogonal polarized optical pulse injection (OPOPI), which deserves further investigation in depth.

In this work, based on the well-known spin flip model (SFM) [29], we numerically study the neuron-like dynamics in VCSELs with OPOPI. At first, we reproduce the experimental findings reported by Hurtado [23]. Then, we go in the following directions. We map the parameter ranges leading to different dynamical response of VCSELs-based neuron by numerical bifurcation analysis. The neuron-like response is also discussed when time-varying pump current is applied. The dependence of spiking frequency on the stimuli strength is further presented for VCSELs with time-varying OPOPI, and the effects of pump current and frequency detuning are examined.

2. Theory

In order to include the OPOPI, we consider a rate equation model for the polarization modes of single-mode VCSELs based on the SFM [15], [20], [29]

$$\frac{dE_x}{dt} = k(1+i\alpha)[(N-1)E_x + inE_y] - (\gamma_a + i\gamma_p)E_x + k_{\text{injx}}E_{\text{injx}}(t)e^{j\Delta\omega_x t} \tag{1}$$

$$\frac{dE_y}{dt} = k(1+i\alpha)[(N-1)E_y - inE_x] + (\gamma_a + i\gamma_p)E_y \tag{2}$$

$$\frac{dN}{dt} = \gamma_N[\mu - N(1+|E_x|^2+|E_y|^2) + in(E_xE_y^* - E_yE_x^*)] \tag{3}$$

$$\frac{dn}{dt} = -\gamma_s n - \gamma_N[n(|E_x|^2+|E_y|^2) + iN(E_yE_x^* - E_xE_y^*)] \tag{4}$$

where E_x and E_y are the amplitudes of XP and YP modes. N is the total carrier inversion between conduction and valence bands, while n is the difference between carrier inversions with opposite spins. k is the field decay rate, $\gamma_a(\gamma_p)$ is the linear dichroism (birefringence), γ_N is the decay rate of N, γ_s is the spin-flip rate, α is the linewidth enhancement factor, and μ is the normalized pump current ($\mu = 1$ is at the threshold). Optical injection is characterized by $E_{\text{injx}}(t)$ and $\Delta\omega_x$. The difference of angular frequency is defined as $\Delta\omega_x = \omega_{\text{inj}} - \omega_0$, where $\omega_0 = (\omega_x + \omega_y)/2$ is the center frequency of two polarization outputs with $\omega_x = \omega_0 + \alpha\gamma_a - \gamma_p$, $\omega_y = \omega_0 + \gamma_p - \alpha\gamma_a$, the frequency detuning between the injected filed and the XP mode is introduced as $\Delta f_x = f_{\text{inj}} - f_x$. Hence, $\Delta\omega_x = 2\pi\Delta f_x + \alpha\gamma_a - \gamma_p$. The input coupling coefficient coincides with k for the ideal case of an effectively mode-matched injected input [18], [29]. The noise is ignored for simplicity. We numerically solve Eqs. (1)-(4) by fourth order Runge-Kutta method using an integration step of 1 ps with typical parameters for 1550 nm VCSELs [20]: $k = 125\,\text{ns}^{-1}$, $\alpha = 2.2$,$\gamma_N = 1\,\text{ns}^{-1}$, $\gamma_s = 1000\,\text{ns}^{-1}$, $\gamma_a = 2\,\text{ns}^{-1}$, $\gamma_p = 192\,\text{ns}^{-1}$, $k_{\text{injx}} = k$, and $\lambda = 1550\,\text{nm}$.

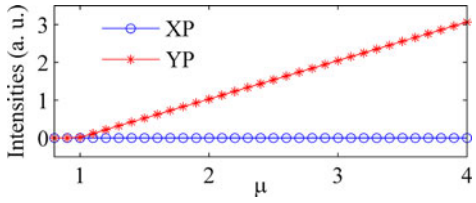

Fig. 1. Polarization-resolved intensities as a function of pump current.

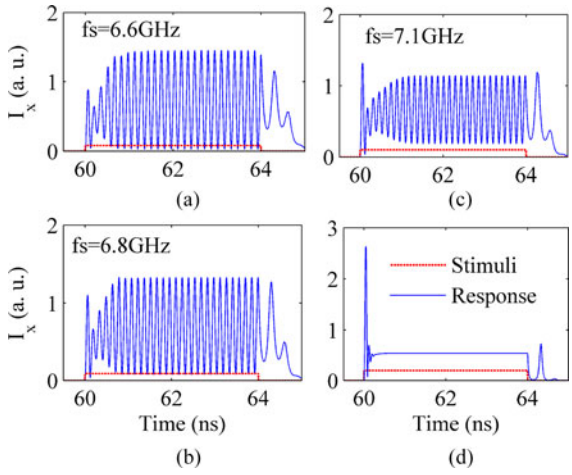

Fig. 2. Response of the XP output for different values of pulse strength. (a) $E_{\text{injx}} = 0.192$, (b) $E_{\text{injx}} = 0.216$, (c) $E_{\text{injx}} = 0.24$, (d) $E_{\text{injx}} = 0.48$, with $\mu = 2.5$, $\Delta f_x = 4\,\text{GHz}$,$f_p = 50\,\text{MHz}$, DT =0.2.

With these parameters, the polarization-resolved intensities as a function of pump current is shown in Fig. 1. Here,$I_{x,y} = |E_{x,y}|^2$, and it can be seen that the YP is the lasing mode and that no polarization switching is observed during the whole range of pump current.

3. Results and Discussion

In this section, first, we numerically reproduce the experimental findings obtained by Hurtado *et al.* in [24], based on a well-known SFM. After that, the operating parameter ranges corresponding to different neuron-like dynamics are revealed by extensive numerical bifurcation analyses. Then, we discuss the effect of time-varying pump current on the response dynamics of VCSEL-based photonic neurons, Finally, the effect of time-varying OPOPI on the neuron-like dynamics of VCSELs and the spiking frequency dependence are examined carefully.

To begin with, we consider an external stimulus of 4ns long rectangular pulse, and try to reproduce the experimental findings obtained in [24]. The repetition frequency of the injecting pulse signal is $f_p = 50\,\text{MHz}$ and duty cycle is DT $= 0.2$. Some representative neuron-like dynamics are presented in Fig. 2. According to the results obtained in [24], the originally depressed mode exhibits more likely to neuron dynamics, hence, we focus on the XP mode here. It can be seen that, when $E_{\text{injx}} = 0.192, 0.216, 0.24$, the response of VCSELs during the 4ns pulse is tonic spiking with multiple periodic pulses, and the spiking frequency f_s, which is defined as the inverse of inter-spike interval, is several gigahertz, which is many orders of magnitude above that observed in biological neuron [28]. In addition, the spiking frequency is higher for larger stimuli strength, which can be attributed to the beating between the injecting filed and the red-shifted cavity mode induced by the external injection [24], [30]. While for $E_{\text{injx}} = 0.48$, a phasic spiking with single abrupt pulse is generated upon the arrival of the stimulus followed by a stable state for the remaining duration of the

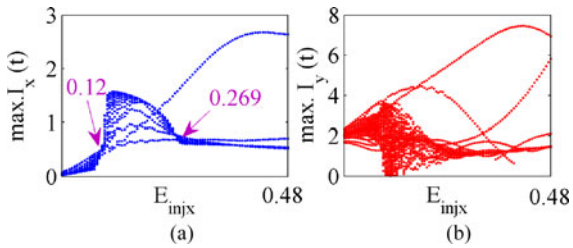

Fig. 3. Bifurcation diagram of (a) XP and (b) YP outputs as functions of E_{injx}. The other parameters are the same as Fig. 2.

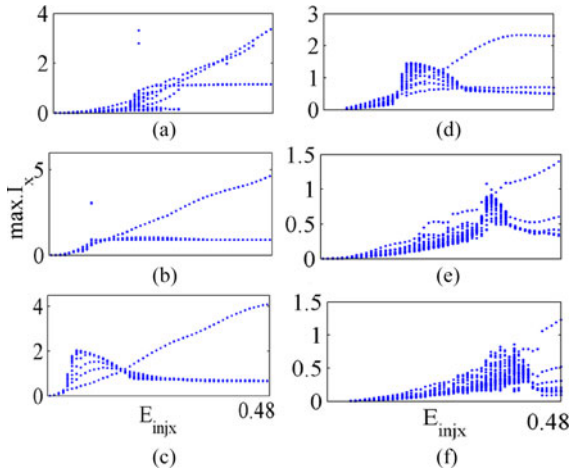

Fig. 4. Bifurcation diagram of XP as functions of E_{injx} under different cases of frequency detuning. (a) $\Delta f_x = -10$ GHz, (b) $\Delta f_x = -5$ GHz, (c) $\Delta f_x = 0$ GHz, (d) $\Delta f_x = 5$ GHz, (e) $\Delta f_x = 10$ GHz, (f) $\Delta f_x = 15$ GHz, and the other parameters are the same as Fig. 2.

injecting pulse. Obviously, these results shown in Fig. 2 agree well with the experimental findings in [24], indicating that the SFM is efficient for numerical analysis of the rich neuron-like dynamics of VCSELs with OPOPI.

To give more insight into the response dynamics, we present the numerical bifurcation diagrams in Fig. 3 by taking the E_{injx} as a controlled variable. Both the XP and YP modes are considered here. It can be seen that, with the increase of E_{injx}, both XP and YP modes co-exist. On the one hand, as shown in Fig. 3(a), small perturbations only lead to a small-amplitude linear response in the originally depressed XP mode for $E_{\text{injx}} < 0.12$. But for $0.12 < E_{\text{injx}} < 0.269$, when the perturbation is sufficiently large, the output of is transferred to an excited firing state. As already shown in Fig. 2(a)–(c), tonic spiking with large amplitude periodic pulses can be generated for these stimuli strengths. With the further increase of the stimuli strength and when $E_{\text{injx}} > 0.269$, phasic spiking with large amplitude single abrupt pulse is generated, and some much smaller amplitude oscillation or constant output can also be observed, as already shown in Fig. 2(d). On the other hand, as shown in Fig. 3(b), the YP mode is not suppressed for all the range of E_{injx}, even with the OPOPI, indicating that the polarization switching is not occurred. Moreover, the dynamical property seems to be more complex than that of XP mode. We also consider the temporal waveforms (not shown here) and find that when the XP mode is not excited, the YP mode keeps constant, when the XP mode is in a firing state, phasic spiking, tonic spiking, quasi-periodic dynamics, as well as chaotic dynamics can be observed for the YP mode, depending on the stimuli strength. As the originally depressed XP mode exhibits more likely to the neurons, we only focus on the dynamics of XP mode in the following.

The bifurcation diagrams for the XP output under different conditions of frequency detuning and pump current are further shown in Figs. 4 and 5, respectively. It can be seen from Fig. 4

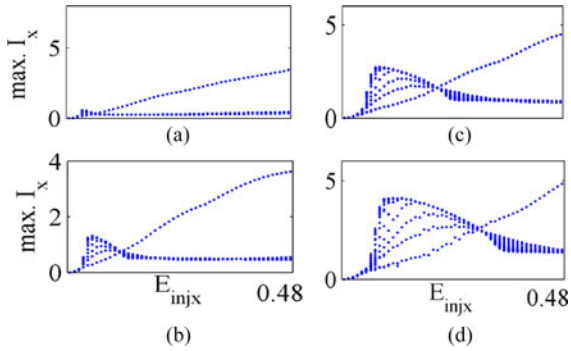

Fig. 5. Bifurcation diagram of XP as functions of E_{injx} under different cases of pump current. (a) $\mu = 1.5$, (b) $\mu = 2$, (c) $\mu = 3$, and (d) $\mu = 4$, with $\Delta f_x = 0$ GHz, $f_p = 50$ MHz, and DT $= 0.2$.

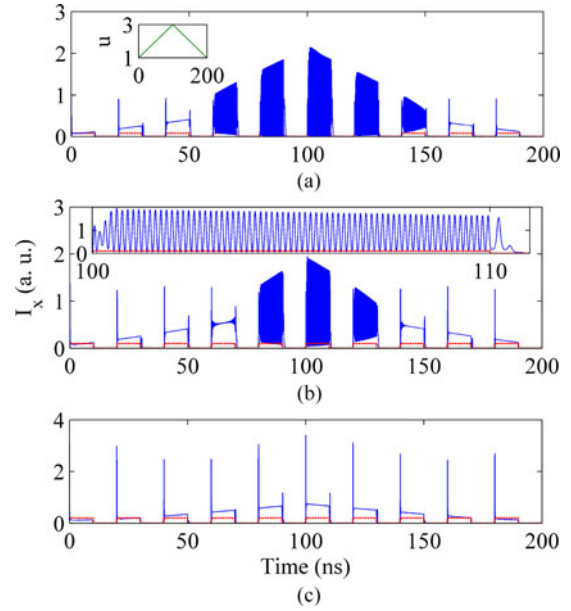

Fig. 6. Response of the XP output for time-varying pump current with fixed optical pulse strength. (a) $E_{\text{injx}} = 0.192$, (b) $E_{\text{injx}} = 0.24$, and (c) $E_{\text{injx}} = 0.48$, with $\Delta f_x = 4$ GHz,$f_p = 50$ MHz, and DT $= 0.5$. The inset in (b) is the enlargement.

that the frequency detuning modifies significantly the bifurcation diagrams, and the range of E_{injx} contributing to the tonic spiking is wider for positive Δf_x and moves to larger value for higher Δf_x. While for negative Δf_x, the region leading to phasic spiking is much wider. On the other hand, as shown in Fig. 5, a large (small) pump current contributes to wider range of E_{injx} corresponding to tonic (phasic) spiking. Hence, to obtain desired neuron-like dynamics in VCSELs, both the frequency detuning and pump current should be carefully adjusted.

Next, we fix the optical injecting pulse strength, and consider the effects of time-varying pump current on the response dynamics of VCSELs-based neuron. Here, three cases of pulse strength are considered, the pump current is continuously increased from 1 to 3 in the time interval of (0, 100 ns), and then decreased continuously from 3 to 1 in the time interval of (100 ns, 200 ns). It can be seen from Fig. 6 that, for $E_{\text{injx}} = 0.192$, rich neuron-like dynamics, such as phasic spiking with single abrupt pulse and tonic spiking with multiple pulses, can also be obtained by continuously adjusting the pump current of VCSELs even with fixed optical injecting pulse strength. As shown in Fig. 6(a), when the pump current is positively scanned, the tonic spiking behavior is occurred

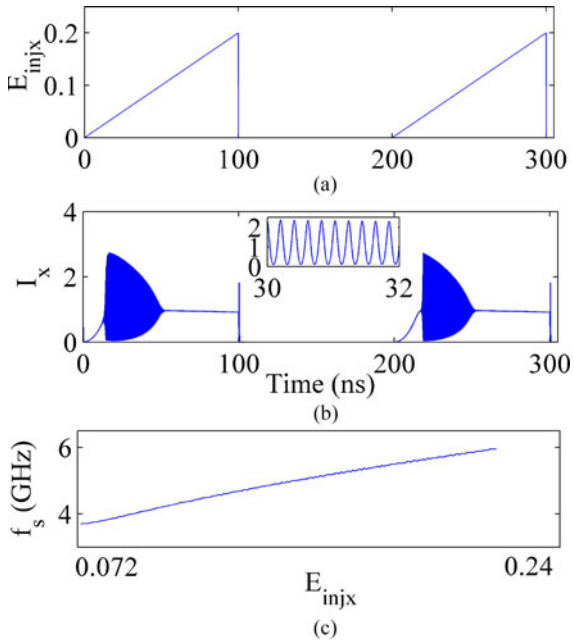

Fig. 7. Temporal waveforms in VCSELs subject to time-varying OPOPI with $f_p = 5$ MHz. (a) E_{injx}, (b) I_x for $\Delta f_x = 0$ GHz, $\mu = 3$. The inset is the enlargement. (c) Spiking frequency f_s as a function of E_{injx}.

for the ranges of $\mu = (2.2, 2.4)$, and $\mu = (2.6, 2.8)$. On the other hand, when the pump current is negatively scanned, the tonic spiking behavior is observed for $\mu = (2.8, 3)$, $\mu = (2.4, 2.6)$, and $\mu = (2, 2.2)$, which exhibits hysteresis property [13], [29]. The corresponding spiking frequency is respectively, $f_s = 6.57, 6.62, 6.67, 6.62, 6.57$ GHz for the five tonic spiking pulse packages. That is to say, the spiking frequency values in different packages are almost the same, indicating that the spiking frequency is not sensitive to distinct pump currents. For $E_{\text{injx}} = 0.24$, the response dynamics are similar, but the tonic spiking range is reduced, and is observed only for $\mu = (2.6, 2.8)$ when the pump current is positively scanned, and is observed for $\mu = (2.8, 3)$ and $\mu = (2.4, 2.6)$ when the pump current is negatively scanned. The spiking frequency for the three tonic spiking pulse packages in Fig. 6(b) is $f_s = 7.14, 7.19, 7.14$ GHz, respectively. For clarity, one representative case of the detailed tonic spiking dynamics is also presented as an inset figure in Fig. 6(b) for $\mu = (2.8, 3)$. For $E_{\text{injx}} = 0.48$, only single abrupt pulse is generated followed by a stable state for all the range of pump current. That is to say, by properly selecting the optical pulse amplitude, the electrically controlled time-varying pump current is also an effective controlled method for achieving different neuron-like dynamics of VCSELs.

Finally, we also consider the effects of time-varying optical injecting pulse on the neuron-like dynamics of VCSELs. Here, we consider $\Delta f_x = 0$ GHz and $\mu = 3$. As shown in Fig. 7(a) and (b), small amplitude linear response is observed for $E_{\text{injx}} < 0.072$. When a critical value is reached, a spike package with different inter-spike intervals is triggered for the range of $0.072 < E_{\text{injx}} < 0.24$. Interestingly, by quantitatively calculating the spiking frequency in that region, we find that, the spiking frequency is monotonically increased with the stimuli strength as shown in Fig. 7(c), which is similar to the spiking frequency dependence observed in VCSELs with saturable absorber [26], in graphene excitable laser [27], as well as in biological neuron [28]. For even stronger injecting pulse strength with $E_{\text{injx}} > 0.24$, the VCSELs is injection-locked to the injecting field, and stable output is observed. At the end of the injecting pulse, some relaxation oscillation pulse is followed, and then the XP output becomes quiescent until the next period of injecting pulse.

We also consider the effects of frequency detuning and pump current on the spiking frequency dependence. The spiking frequency values as a function of E_{injx} for different cases of frequency detuning are shown in Fig. 8. It is shown that the aforementioned spiking frequency dependence

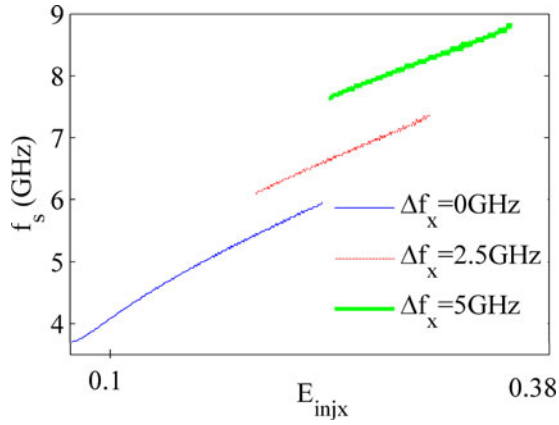

Fig. 8. Spiking frequency f_s as a function of E_{injx} for different cases of frequency detuning with $\mu = 3$.

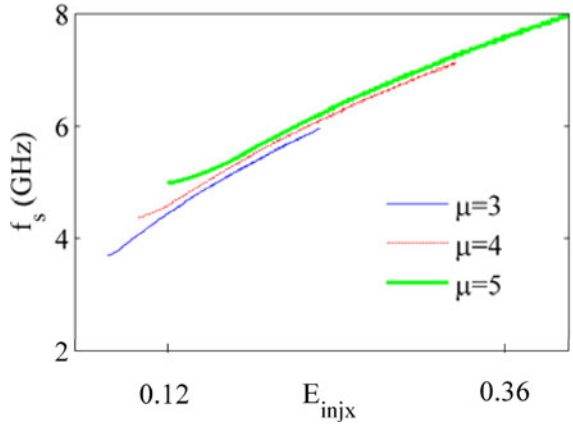

Fig. 9. Spiking frequency f_s as a function of E_{injx} for different pump currents with $\Delta f_x = 0$ GHz.

can be observed for all the considered conditions. For $\Delta f_x = 0$ GHz, the spike package is observed in the range of $E_{\text{injx}} \in (0.074, 0.238)$, and the spiking frequency is increased almost linearly from $f_s = 3.7$ GHz to $f_s = 5.95$ GHz. For $\Delta f_x = 2.5$ GHz, the spike package is observed in the range of the $E_{\text{injx}} \in (0.192, 0.305)$, and the spiking frequency is increased almost linearly from $f_s = 6.1$ GHz to $f_s = 7.35$ GHz. For $\Delta f_x = 5$ GHz, the spike package is observed in the range of the $E_{\text{injx}} \in (0.24, 0.36)$, and the spiking frequency is increased almost linearly from $f_s = 7.63$ GHz to $f_s = 8.85$ GHz. That is to say, the range of E_{injx} corresponding to spike package behavior moves to higher E_{injx} for large positive Δf_x, and the values of f_s are also higher for larger Δf_x.

Correspondingly, the spiking frequency values as functions of E_{injx} for different pump currents are shown in Fig. 9. It can be seen that, similar spiking frequency dependence can be observed for all the considered pump currents. Large pump current leads to wider range of E_{injx}, corresponding to spike package behavior, and the values of f_s are also slightly higher.

To the best of our knowledge, such spiking frequency dependence in photonic neuron based on VCSELs with OPOPI has not yet been reported, which opens the possibility for spiking frequency coding for neuro-inspired photonic information processing.

4. Conclusion

In summary, based on the well-known SFM of VCSELs, several neuron-like dynamics, such as phasic spiking with single abrupt pulse, and tonic spiking with multiple periodic pulses, are reproduced in 1550 nm VCSELs subject to OPOPI. The numerical bifurcation analysis further indicates

that pump current and frequency detuning are two key parameters for the neuron-like dynamics in VCSELs. A large pump current and positive frequency detuning are the benefit for wider tonic spiking range, while small pump current and negative frequency detuning favor wider range of phasic spiking behavior. Moreover, by carefully selecting the optical injecting pulse strength, different neuron-like dynamics can also be observed when the time-varying pump current is applied. Finally, we find that the spiking frequency is monotonically increased with the stimuli strength when time-varying optical injecting pulse is introduced, which opens the possibility for spiking frequency coding in photonic neuron based on VCSELs with OPOPI, and are interesting and valuable for the ultrafast photonic neuromorphic systems and brain-inspired photonic information processing.

References

[1] K. S. Kravtsov, M. P. Fok, P. R. Prucnal, and D. Rosenbluth, "Ultrafast all-optical implementation of a leaky integrate-and-fire neuron," *Opt. Exp.*, vol. 19, no. 3, pp. 2133–2147, Jan. 2011.

[2] M. A. Nahmias, B. J. Shastri, A. N. Tait, and P. R. Prucnal, "A leaky integrateand- fire laser neuron for ultrafast cognitive computing," *IEEE J. Sel. Topics Quantum Electron.*, vol. 19, no. 5, Sep./Oct. 2013, Art. no. 1800212.

[3] F. Selmi, R. Braive, G. Beaudoin, I. Sagnes, R. Kuszelewicz, and S. Barbay, "Relative refractory period in an excitable semiconductor laser," *Phys. Rev. Lett.*, vol. 112, no. 18, May 2014, Art. no. 183902.

[4] F. Selmi, R. Braive, G. Beaudoin, I. Sagnes, R. Kuszelewicz, and S. Barbay, "Temporal summation in a neuromimetic micropillar laser," *Opt. Lett.*, vol. 40, no. 23, pp. 5690–5693, Dec. 2015.

[5] P. R. Prucnal, B. J. Shastri, T. F. D. Lima, M. A. Nahmias, and A. N. Tait, "Recent progress in semiconductor excitable lasers for photonic spike processing," *Adv. Opt. Photon.*, vol. 8, no. 2, pp. 228–299, Jun. 2016.

[6] E. C. Mos, J. J. L. Hoppenbrouwers, M. T. Hill, M. W. Blum, J. J. H. B. Schleipen, and H. D. Waardt, "Optical neuron by use of a laser diode with injection seeding and external optical feedback," *IEEE Trans. Neural Netw.*, vol. 11, no. 4, pp. 988–996, Jul. 2000.

[7] M. Turconi, B Garbin, M Feyereisen, M Giudici, and S Barland, "Control of excitable pulses in an injection-locked semiconductor laser," *Phys. Rev. E*, vol. 88, no. 2, Aug. 2013, Art. no. 022923.

[8] B. Garbin, D. Goulding, S. P. Hegarty, G. Huyet, B. Kelleher, and S. Barland, "Incoherent optical triggering of excitable pulses in an injection-locked semiconductor laser," *Opt. Lett.*, vol. 39, no. 5, pp. 1254–1257, Mar. 2014.

[9] S. Barbay, R. Kuszelewicz, and A. M. Yacomotti, "Excitability in a semiconductor laser with saturable absorber," *Opt. Lett.*, vol. 36, no. 23, pp. 4476–4478, Dec. 2011.

[10] W. Coomans, L. Gelens, S. Beri, J. Danckaert, and G. V. Sande, "Solitary and coupled semiconductor ring lasers as optical spiking neurons," *Phys. Rev. E*, vol. 84, no. 3, Sep. 2011, Art. no. 036209.

[11] T. V. Vaerenbergh, K. Alexander, J. Dambre, and P. Bienstman, "Excitation transfer between optically injected microdisk lasers," *Opt. Exp.*, vol. 21, no. 23, pp. 28922–28932, Nov. 2013.

[12] B. Romeira, F. Kong, J. M. L. Figueiredo, J. Javaloyes, and J. Yao, "High-speed spiking and bursting oscillations in a long-delayed broadband optoelectronic oscillator," *J. Lightw. Technol.*, vol. 33, no. 2, pp. 503–510, Jan. 2015.

[13] W. L. Zhang, W. Pan, B. Luo, X. H. Zou, and M. Y. Wang, "Polarization switching and hysteresis of VCSELs with time-varying optical injection," *IEEE J. Sel. Top. Quantum Electron.*, vol. 14, no. 3, pp. 889–894 , May/Jun. 2008.

[14] S. Y. Xiang *et al.*, "Influence of polarization-mode-competition on chaotic unpredictability of vertical-cavity surface-emitting lasers with polarization-rotated optical feedback," *Opt. Lett.*, vol. 36, no. 3, pp. 310–312, Feb. 2011.

[15] R. A. -Seyab, K. Schires, N. A. Khan, A. Hurtado, I. D. Henning, and M. J. Adams, "Dynamics of polarized optical injection in 1550-nm VCSELs: theory and experiments," *IEEE J. Sel. Topics Quantum Electron.*, vol. 17, no. 5, pp. 1242–1249, Sep./Oct. 2011.

[16] S. Y. Xiang, W. Pan, B. Luo, L. Yan, X. Zou, and N. Li, "Influence of variable-polarization optical feedback on polarization switching properties of mutually-coupled VCSEL," *IEEE J. Sel. Topics Quantum Electron.*, vol. 19, no. 4, Jul./Aug. 2013, Art. no. 1700108.

[17] Y. Hong, "Experimental study of time-delay signature of chaos in mutually coupled vertical-cavity surface-emitting lasers subject to polarization rotated optical injection," *Opt. Exp.*, vol. 21, no. 15, pp. 17894–17903, Jul. 2013.

[18] P. Pérez, A. Valle, L. Pesquera, and A. Quirce, "All-optical inverter based on polarization switching in VCSELs subject to single and dual optical injection," *IEEE J. Sel. Topics Quantum Electron.*, vol. 19, no. 4, Jul./Aug. 2013, Art. no. 1700408.

[19] Z. Q. Zhong, Z. M. Wu, J. G. Wu and G. Q. Xia, "Time-delay signature suppression of polarization-resolved chaos outputs from two mutually coupled VCSELs," *IEEE Photon. J.*, vol. 5, no. 2, Apr. 2013, Art. no. 1500409.

[20] M. F. Salvide, M. S. Torre, I. D. Henning, M. J. Adams, and A. Hurtado, "Dynamics of normal and reverse polarization switching in 1550-nm VCSELs under single and double optical injection," *IEEE J. Sel. Topics Quantum Electron.*, vol. 21, no. 6, Nov./Dec. 2015, Art. no. 1800309.

[21] Z.-Q. Zhong, Z.-M. Wu, J. Song, L. Y. Wang, T. Deng, and G.-Q. Xia, "Polarization dynamics of 1550-nm VCSELs subject to polarization-preserved FBG feedback," *IEEE Photon. Technol. Lett.*, vol. 28, no. 9, pp. 963–966, May 2016.

[22] A. Quirce *et al.*, "Polarization switching and injection locking in vertical-cavity surface-emitting lasers subject to parallel optical injection," *Opt. Lett.*, vol. 41, no. 11, pp. 2664–2667, Jun. 2016.

[23] A. Hurtado, I. D. Henning, and M. J. Adams, "Optical neuron using polarization switching in a 1550 nm-VCSEL," *Opt. Exp.*, vol. 18, no. 24, pp. 25170–25176, Nov. 2010.

[24] A. Hurtado, K. Schires, I. D. Henning, and M. J. Adams, "Investigation of vertical cavity surface emitting laser dynamics for neuromorphic photonic systems," *Appl. Phys. Lett.*, vol. 100, no. 10, Mar. 2012, Art. no. 103703.

[25] A. Hurtado and J. Javaloyes, "Controllable spiking patterns in long-wavelength vertical cavity surface emitting lasers for neuromorphic photonics systems," *Appl. Phys. Lett.*, vol. 107, no. 24, Dec. 2015, Art. no. 241103.
[26] T. Elsass, K. Gauthron, G. Beaudoin, I. Sagnes, R. Kuszelewicz, and S. Barbay, "Control of cavity solitons and dynamical states in a monolithic vertical cavity laser with saturable absorber," *Eur. Phys. J. D.*, vol. 59, no. 1, pp. 91–96, Jul. 2010.
[27] B. J. Shastri, M. A. Nahmias, A. N. Tait, A. W. Rodriguez, B. Wu, and P. R. Prucnal, "Spike processing with a graphene excitable laser," *Sci. Rep.*, vol. 6, Jan. 2016, Art. no. 19126.
[28] E. M. Izhikevich, "Neural excitability, spiking and bursting," *Int. J. Bifur. Chaos*, vol. 10, no. 6, pp. 1171–1266, Jun. 2000.
[29] J. M. Regalado, F. Prati, M. S. Miguel, and N. B. Abraham, "Polarization properties of vertical-cavity surface-emitting lasers," *IEEE J. Quantum Electron.*, vol. 33, no. 5, pp. 765–783, May 1997.
[30] C.-H. Chang, L. Chrostowski, and C. J. C. -Hasnain, "Injection locking of VCSELs," *IEEE J. Sel. Topics Quantum Electron.*, vol. 9, no. 5, pp. 1386–1393, Sep./Oct. 2003.